Applied Physics Research; Vol. 6, No. 6; 2014
ISSN 1916-9639 E-ISSN 1916-9647
Published by Canadian Center of Science and Education

Investigation of Precision Large-Caliber Slot Cutting of Sheet Steel Using Single-Mode Fiber Laser Radiation

A. M. Soroka[1], V. P. Panchenko[2], A. A. Vitshas[1], A. G. Zelentsov[1], K. S. Kravchuk[3], V. P. Menakhin[1] & A. V. Yakson[1]

[1] Strazh-Laser Company, s. Besedy, Leninskiy region, Moscow oblast, 142715, Russia

[2] Troitsk Institute for Innovation and Fusion Research, ul.Pushkovykh 12, Troitsk D.C., Moscow, Russia

[3] Technological Institute for Superhard and Novel Carbon Materials, ul.Tsentralnaya 7a, Troitsk D.C., Moscow, Russia

Correspondence: A. M. Soroka, Strazh-Laser Company, s. Besedy, Leninskiy region, Moscow oblast, 142715, Russia. E-mail: ark.soroka@yandex.ru

V.P. Panchenko, Troitsk Institute for Innovation and Fusion Research, ul.Pushkovykh 12, Troitsk D.C., Moscow, 142190, Russia. E-mail: panchvictor@gmail.com

Received: October 9, 2014 Accepted: October 26, 2014 Online Published: November 3, 2014

doi:10.5539/apr.v6n6p45 URL: http://dx.doi.org/10.5539/apr.v6n6p45

Abstract

We present results of the experimental and theoretical investigation of the characteristics and features of precision large-caliber slot cutting of low-carbon steel sheets with thicknesses up to 10 mm by radiation of 1-kW single-mode fiber laser. Using periodic-pulsed single-mode laser radiation and oxygen as the cutting gas, slots with calibers from 20 to 60 (in some cases – up to 100) and widths up to about 60 microns have been obtained. The cutting speed (50—100 mm/min) was measured and the efficiency of precision cutting (≈3%) and efficiency of laser radiation transport in the waveguide mode (≈25%) were estimated. The morphology and roughness parameters of the cut surface were determined. Variation of the hardness and phase structure of steel in the direction of normal to the slot wall were studied. A qualitative model of laser oxygen precision slot cutting with deep channeling is proposed.

Keywords: laser cutting, fiber laser, precision cutting, mild steel, experiment, speed of cutting, width of slot, caliber of slot, surface of cut, roughness, SPMtopography image, hardness, phase structure, analysis, physical model

1. Introduction

Commercial technological CO_2 lasers do not allow slotted holes and round cuts to be obtained with curvature radii below about 250 μm, while the slot caliber $K=h/b$ typically does not exceed 20 (where b is the slot width and h is its depth that is equal to sheet thickness in case of sheet material cutting). Using laser cutting setups based on few-mode ytterbium-doped fiber and disk lasers operating on a 1.07 μm wavelength at a power of up to 5 kW and efficiency of about 30% (which principally differ from gas lasers), it is possible to obtain 150—250 μm wide slotted holes in metal sheets in the lasergas cutting regime (Trumpf Co., 2012; Morgenthal, 2012; IPJ in the News, 2014). The slot caliber typically amounts to $K\approx20$, the laser radiation propagates in the slot with low losses according to the laws of geometric optics, and the cutting gas pressure is sufficient to blow melted metal away from the cut zone (Gladush & Smurov, 2011).

In the case of deeper channeling (with $K\geq30$), the process of metal cutting is sharply complicated as a result of both the strong attenuation of laser radiation in the waveguide regime of propagation in a slotted channel (Gladush & Smurov, 2011) and the low pressure of the cutting gas (caused by large hydraulic losses), which becomes insufficient to blow melted metal away from the cut zone.

In this context, we posed a task of experimentally checking the possibility of obtaining slotted holes with $K\geq 30$ during laser gas cutting with few-mode or single-mode fiber laser radiation, determining conditions necessary for this result, and constructing a physico-mathematical model of the process.

This paper presents most complete results of the experimental and theoretical investigation of the specific features and characteristics of precision large-caliber slot cutting of low-carbon steel sheets by radiation of 1-kW single-mode fiber laser, which were previously reported in brief (Vitshas et al., 2014).

2. Experiment

2.1 Experimental Setup and Conditions of Investigation

The experiments were performed on a setup (Vitshas et al., 2014) that was specially designed and constructed for studying the interaction of radiation of a single-mode fiber laser with metals and for obtaining small-size slotted holes with large calibers ($K \geq 30$) in steel blanks and articles. The setup is based on a single-mode ytterbium-doped fiber laser generating radiation with a wavelength of $\lambda = 1.07$ μm at a power of 1 kW and beam quality parameter $M^2 < 1.2$, which is capable of operating in both the continuous-wave and periodic-pulsed regime with controlled on/off ratio (IPJ in the News, 2014). The laser radiation is fed via a fiber cable into an immobile cutting head (Presitec), which is mounted vertically on aerodynamic supports above a mobile work table. The laser cutting head contains a collimator with a focal distance of 60 mm and a beam aperture of $D_a = 8$ mm, a lens with a focal distance of $F = 200$ mm, and a convergent conical nozzle with output diameter 1 mm for obtaining a cutting gas jet coaxial with the laser beam. The output radiation beam is directed along the conical nozzle axis (axis z) perpendicular to the surface of a processed object and focused into a spot with diameter $d_f \approx 30$ μm. The focal spot position can be shifted from +5 mm to –5 mm relative to the object surface. The distance from the laser cutting head edge to the surface of a metal sheet was within 0.5—0.7 mm.

In experiments, we have varied the laser pulse power, the repetition rate and on/off ratio of laser pulses, the thickness of steel sheets (1.5 to 12 mm), the cutting gas type (oxygen, air, nitrogen) and pressure (0.2 to 1.5 MPa), and the focal spot position relative to the sheet surface ($z = 0$ to –4 mm, where minus implies that the focus is shifted down below the surface).

2.2 Experimental Investigation of Precision Laser Gas Cutting

We have studied the cutting of slotted holes and contours of arbitrary shape in low-carbon steel (St3 grade) sheets with thicknesses from 1.5 to 12 mm. In addition, we have also studied the cutting of 4-mm-thick stainless steel sheet in order to obtain a slotted cut of minimum width with high surface quality. As a result, we obtained reproducible experimental data on the conditions of optimum fiber-laser cutting of small-size slotted holes with calibers up to $K = 60$, which are summarized in Table 1. In separate experiments the slot caliber reached up to $K = 80$. The error of reproducible cutting holes of complicated shape with a characteristic diameter of ≈ 1 mm was ±5%.

Table 1. Main parameters of optimum slot cutting of sheet steel by fiber laser radiation with oxygen as the cutting gas

Sheet thickness h, mm	Laser pulse power, P_l	Pulse repetition rate, Hz	Pulse on/off ratio	Gas pressure, atm	Laser focal spot level, mm	Cuttingspeed, mm/ min	Cut width on input (b_1) / output (b_2)surface, μm/μm	Slot caliber $K = h/b$
1.5	200	150-250	3	8-4	0	100	80/70	20
2.0	300	250	3	8-4	0	70	100/60	25
3.0	400	110	3	8-4	0	70	130/110	25
5.0	900	120	3	4	-2	60	140/120	39
6.0	900	120	3-4	3-4.5	(0)-(-1)	60	145/120	45
8.0	930	125-150	2.5-3	2.5	-1	50	150/130	57
10.0	950	120	2	5-6.5	(-1)-(2)	20	200/170	57
Stainless steel4.0	910	245	6	3.5	0	30	80/60	57

Based on the obtained experimental results, it was established that

(i) Precision cutting of small-size (~100 μm) slotted holes of arbitrary shape with large slot calibers ($K \geq 30$) is only possible using single-mode fiber laser radiation;

(ii) Precision laser cutting is not realized using few-mode laser radiation;

(iii) Precision cutting is possible only with oxygen as the cutting gas, which means that the process has a clearly pronounced laser-thermochemical character;

(iv) For each thickness of steel sheet, there is an optimum set of main parameters which determine the ultimate (maximum) slot caliber, minimum slot width, and maximum cutting speed;

(v) Precision cutting is only realized in a periodic-pulsed regime of fiber laser operation with optimum on/off ratio within 2—4 and pulse repetition rates from 250 Hz (for h = 1.5 mm) to 120 Hz (for h = 10 mm), so that the duration of minimal radiation action on the metal is τ_{rad} = 2—3 ms, while the optimum radiation pulse power increases with the sheet thickness;

(vi) The cutting speed at a large slot caliber (K > 20) is small as compared to that for high-power CO_2 lasers and ytterbium-doped fiber lasers, strongly depends on the sheet thickness, and varies from 100 mm/min (h = 1.5 mm, K = 20) to 50 mm/min (h = 8 mm, $K \approx 60$);

(vii) As the average radiation power decreases due to a decrease in the on/off ratio and/or passage to a stationary regime, the cutting speed increases, but this is accompanied by significant increase in the slot width which approaches a level (~300 μm) typical of standard technological lasers.

(viii) The slotted cut has a wedge shape with relative convergence $\alpha = (b_2—b_1)/(2h)$ along the beam, which decreases from 10^{-2} to 10^{-3} with increasing sheet thickness;

(ix) Permissible oxygen pressure is limited from below on a level of 0.25 MPa;

(x) Cut surface exhibits anisotropic roughness in the form of grooves oriented along the sheet thickness, predominantly along the beam (axis z, Figure 1). In the uppermost surface layer (to a depth of ≈30% of the sheet thickness), the traces of melted metal are vertical and parallel to each other, while somewhat deeper they are declined (by angle up to 10°) and transformed into periodic curvilinear comb-like wavy structures the period of which increases with the depth (Figure 1);

(xi) The cut surface color is different in two regions, being light-yellow down to a depth of about 30% of the sheet thickness and changing to gray (with yellow inclusions) in the remainder of the layer thickness (Figure 1).

(xii) The slotted hole retains a small amount of agglomerated slag of gray color, with irregular shape and a maximum size of about slot width b.

The morphology and roughness of the cut surface were determined on square samples cutfrom a steel sheet with a thickness of 8 mm. The parameters of roughness were measured using a profilometer on 8-mm-long base along five tracks (*1*—*5*, Figure 1) in the direction of cutting (axis x).

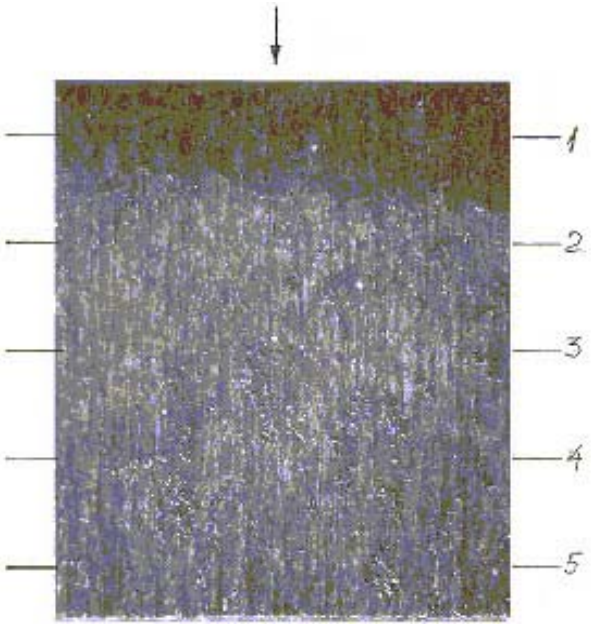

Figure 1. General view and arrangement of tracks (*1*--*5*) used for determining roughness parameters on face 4 of 8-mm-thick low-carbon steel sheet sample

Table 2 presents values of the arithmetic mean profile deviation and roughness step (wavelength) for the five tracks studied. The values of main roughness parameters determined on the other three faces of the sample differed rather insignificantly.

Table 2. Main parameters of the cut surface roughness determined on sample face 4

Track number, face 4	Arithmetic mean profile deviation $<R_a>$, μm	Average step (wavelength) of roughness profile, $<S_m>$, μm
1	5.42	147
2	6.99	164
3	9.75	229
4	10.2	264
5	12.7	225

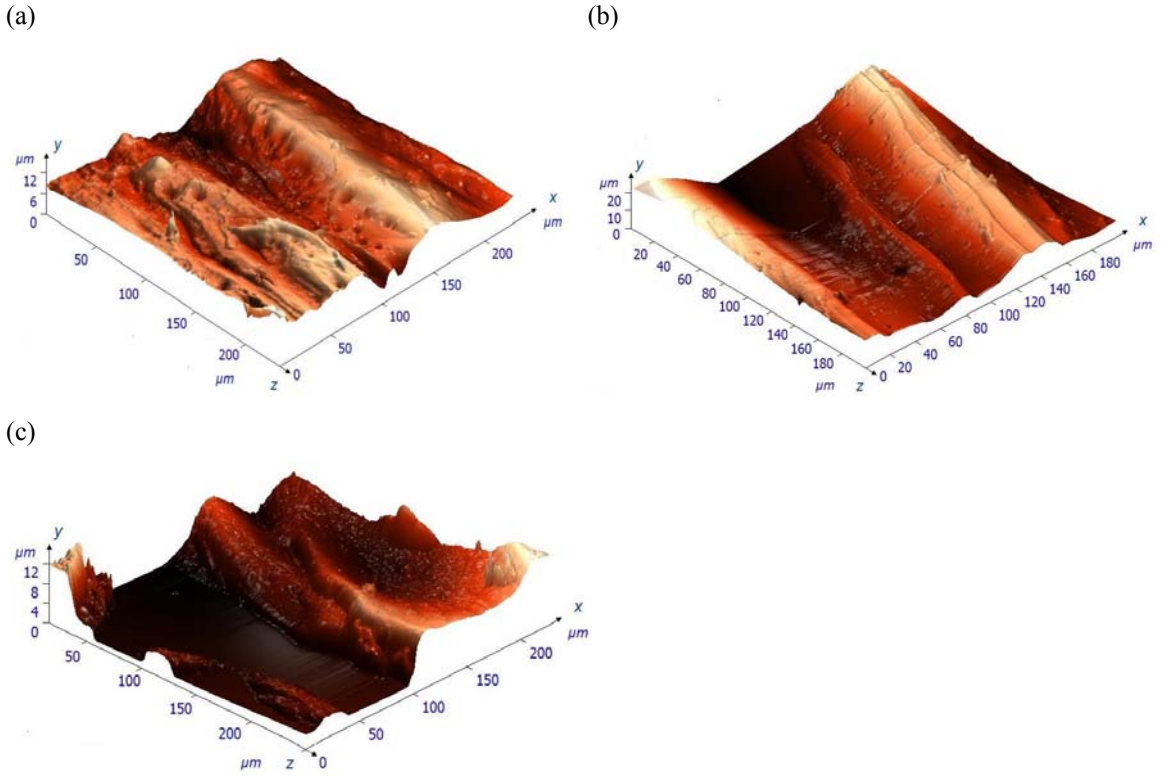

Figure 2. SPM images of the cut surface relief at the middle of (a) track *1*, (b) track *3*, and (c) track *5* indicated in Figure 1

It is a characteristic feature that, in the upper region of the cut surface with length h_1=(0.2—03)h along axis z (zone I corresponding to the light-yellow region in Figure 1), the profile deviation and roughness height are 1.5—2 times smaller than in the region of waveguide propagation of laser radiation (tracks *3*—*5*). The average step (wavelength) of the roughness profile varies from ≈150 to ≈270 μm. The roughness height does not exceed 15 μm, which sometimes eliminates the need for subsequent processing of the cut surface.

The surface morphology of the cut surface was studied by taking sequential images along two tracks in the beam direction (upside down) and two tracks in the lateral direction (tracks *1* and *5* in Figure 1) with the aid of an atomic force microscope with x500 magnification.

Images of the cut surface relief obtained with the aid of scanning probe microscopy (SPM) and the variation of this relief in depth, together with variation of the surface color, are indicative of different regimes of laser cutting in the top and bottom parts of a processed sheet (Vitshas et al., 2014). The periodic wavy structure observed on the cut surface in the direction of cutting (axis x), which consists of hills and troughs (Figures 2a—2c), is caused by the periodic-pulsed regime of cutting that leads to pulsed ejection of melted metal into the slotted channel and its solidification in boundary layers on the slot walls. The parameters of roughness determined using SPM images of the surface relief mostly agree with the data of profilometry (Table 2).

The SPM images of various regions in the cut surface relief revealed the presence of a small amount of previously unreported local small-scale formations in the form of craters and cone-shaped protrusions (peaks) with diameters

of 10—20 μm and heights within 5—10 μm (Figure 2). These objects are chaotically arranged and their axes are oriented parallel to axis *y* rather than perpendicular to the metal surface at the site of occurrence. The number of these local peaks and especially the number of craters rapidly decrease with increasing cut depth. These objects are apparently formed as a result of the interaction of liquid metal drops with solidifying melt on the slot wall.

For comparative evaluation of the quality of cut surface, we have performed cutting of the analogous steel sheet by continuous radiation of a CO_2 laser complex BySprint at a power of 3 kW (Vitshas et al., 2014). It was established that the surface morphology of the cut surface was qualitatively similar to that obtained by fiber laser cutting. However, the step of the longitudinal periodic structure (along axis *x*) was much greater and increased in depth from $<S_m>$=220 μm to$<S_m>$=430 μm. In addition, the cut surface also contained local small-scale formations analogous to those described above.

The established distinctive features of the character of laser cutting by single-mode fiber laser suggest that the upper zone I of the cut surface within length h_1 is formed mostly under the action of radiation with high power density propagating according to the laws of geometric optics (Vitshas et al., 2014). This is also confirmed by the light-yellow color of the cut surface, which is caused by intense oxidation of the metal surface (Figure 1).

In order to estimate the degree of thermal action (surface quenching and/or self-tempering) upon material in the cut zone, we have measured the hardness distribution and determined the phase structure of steel on the surfaces of sheet, cut, and sections made at various distances from the cut surface. The results of hardness measurements on various surfaces are presented in Figure 3.

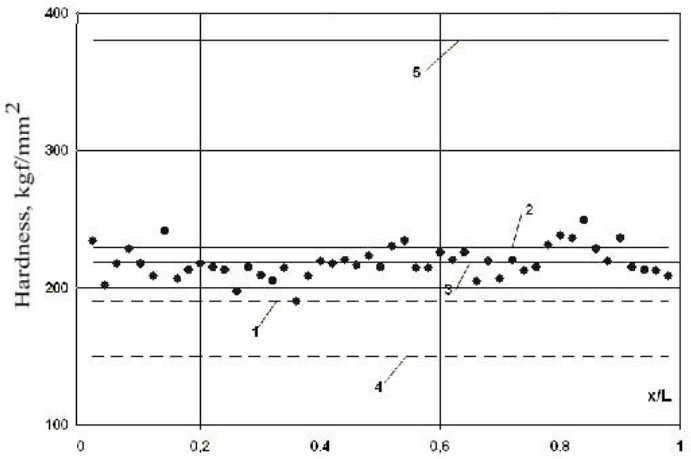

Figure 3. Hardness distribution in the direction of cutting for various surfaces of the sample presented in Figure 1: (*1*) average hardness of the initial sheet surface; (*2*) average hardness on the cut surface; (*3*) average hardness and (points •) local values along track *3*; (*4*) average hardness on the surface of section at a depth of 1 mm from the cut surface; (5) average hardness for track *3* on the cut surface made by CO_2 laser (1 kgf/mm^2 = 1 HB = 9.81 MPa)

The average surface hardness of the initial (unprocessed) steel sheet was 190 kgf/mm^2 (Figure 3, line *1*). The phase structure of steel on the sheet surface was isotropic, with equiaxial ferrite grains and small (up to 20%) pearlite inclusions on the grain boundaries (Figure 4a). The average surface hardness measured on the section made at a depth of 1 mm from the sheet surface was 149 kgf/mm^2.

The hardness of metal on the cut surface was measured at 50 points on the tracks *1*, *3*, and *5* (Figure 1) in the direction of cutting. The average hardness on the cut surface was 229 kgf/mm^2 at a high homogeneity of ±10% (Figure 3, line *2*). The average hardness for 50 points on track *3* (Figure 1) was 218 ± 26 kgf/mm^2 (Figure 3, line 3). The phase structure of the cut steel changed rather insignificantly, as manifested by the appearance of ferrite grains with dimensions from 5 to 30 μm (Figure 4b).

By removal of sequential metal layers parallel to the cut surface and measurement of hardness along three tracks in the obtained sections, it was established that the hardness exhibits stabilization on a level of 152 ± 14 kgf/mm^2 at a depth of 1 mm (line *4,* Figure 3), where the phase structure is close to that of steel on the sheet surface (Figure 4a). This state of the metal, which agrees with data on the hardness and structure at a depth of 1 mm from the sheet surface, should be considered as an unperturbed core with the hardness about 1.2 times smaller than that on the sheet surface.

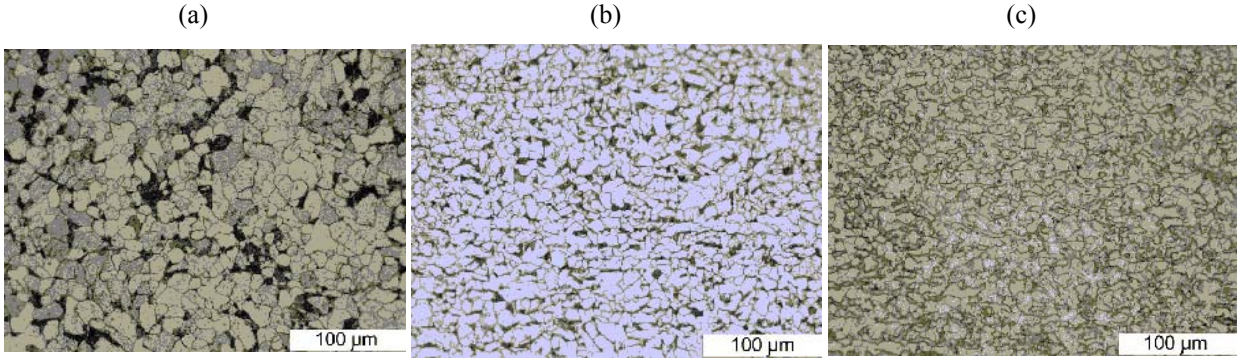

Figure 4. Phase structure of steel on the (a) initial sheet surface and (b, c) cut surface upon cutting with fiber laser and CO_2 laser, respectively (magnification, x500)

Therefore, the fiber laser cutting is accompanied by thermal action to a depth of ≈1 mm, which agrees with the estimation of the thermal wave propagation depth as $\sqrt{(4\cdot\chi_c\cdot b/v_c)} \approx 1$ mm for experimental values of the cutting speed ($v_c \approx 1$ mm/s, $b \approx 100$ μm), by insignificant (1.2-fold) increase in the hardness (quenching) of the cut surface relative to the sheet surface, and by 1.5-fold increase in the hardness relative to that in the core. This is related to the fact that, in the waveguide regime of radiation transport, the cut surface over the entire slot depth occurs under the periodic-pulsed action of laser radiation for a relatively long time due to the low cutting speed.

For a time period of $\tau_{rad} = \Delta x/v_c \approx 200$ ms, which is spent for cutting through a metal sheet with thickness h in experiment on determining the cutting speed v_c (see below), the thermal wave penetrates in depth of the metal by a characteristic distance of ≈2.5 mm that is ≈6 times greater than in the case of cutting by CO_2 laser radiation. This leads to a relatively slow heating and cooling of the surface layers of steel and, hence, results in their strengthening (quenching) to a lesser degree. The values of dimensionless power $Be_1 = \langle P_l \rangle/(h\cdot\lambda_c\cdot T_c') \approx 0.5$ and Peclet number $Pe = v_p\cdot b/\langle\chi_c\rangle \approx 0.01$ are also significantly lower than those for CO_2 laser cutting (1.6 and 0.6, respectively) (Malikov, Orishich, & Shulyat'ev, 2012).

Analogous investigation of the cut surface upon CO_2 laser cutting showed that the hardness of this surface exhibited significant growth in the direction of radiation propagation (upside down) from the average value of 170 kgf/mm^2 on a track passing 1 mm below the sheet surface to 379 kgf/mm^2 (Figure 3, line 5) on the bottom track passing 1 mm above the rear surface. At the same time, the steel structure changes from the isotropic fine-grained "ferrite (50%)—pearlite" phase (Figure 4a) to "pearlite (90%)—ferrite" phase (Figure 4c).

The results of hardness measurements on the surfaces of sections showed that, already at a distance of 0.5 mm from the cut surface, the hardness approaches its value (140 kgf/mm^2) in the core of the sheet, which is 30% lower than on the sheet surface. The steel structure in the core represents the isotropic fine-grained "ferrite (50%)—pearlite" phase. Therefore, the scale of thermal action in depth of the metal in the case of cutting by CO_2 laser radiation has a characteristic length of ≈0.5 mm, which agrees with the estimated length of thermal wave propagation $\sqrt{(4\cdot\chi_c\cdot b/v_c)} \approx 0.4$ mm ($v_c \approx 50$ mm/s, $b \approx 300$ μm, $Pe \approx 1.5$).

For subsequent estimations, we use experimental values of the pulse repetition rate $\nu_p \approx 120$ Hz, on/off ratio ≈3, and cutting speed $v_c \approx 0.9$ mm/s. The characteristic size (step) Δx in the direction of cutting (axis x) is close to the scale of inhomogeneity (roughness wavelength) S_m, and the experimental data confirm that $\Delta x \sim S_m \sim b$. Then, the number of cycles necessary for cutting a metal through thickness $h_2 = h - h_1$ is $N_c = \Delta x\cdot\nu_p/v_c \approx 30$, the cycle duration is $\tau_1 \approx 1/\nu_p \approx 8.3$ ms, the radiation pulse duration per cycle is $\tau_{rad} \approx 2.8$ ms, and the pause between pulses amounts to 5.5 ms. The thickness of cut (removed) metal per cycle is $\Delta z_1 \approx h_2/N_c \approx 200$ μm and the time of cutting through the entire sheet thickness is ≈250 ms. Note that, for this time, the sheet travels a distance of ≈200 μm in the direction of cutting. However, due to a small size of the focal spot and the waveguide regime of laser radiation propagation, the radiation power density is sufficient to cut metal in the bottom part of the slot.

The useful power of incident laser radiation—i.e., the laser power ratio to volume flow rate of the cut (removed) metal—amounts to $w_l = \langle P_l \rangle/(h\cdot b\cdot v_c) \approx 7\cdot10^{11}$ J/m^3 and is approximately (to within 20%) constant for all thicknesses of low-carbon steel sheets studied.

3. Analysis of Experimental Results and Construction of a Model of Precision Laser Cutting

The investigation of cut surfaces revealed the existence of characteristic regions in depth of the slot as well as characteristic scales of roughness and profile inhomogeneity (waviness) step in the direction of cutting (axis x),

which are on the order of the cut width $\Delta x \approx b$. This circumstance suggests that the melting of a metal layer and its removal from the slot proceed with the formation of a "step" (trough or shelf) that propagates in the direction of laser beam (axis z) upside down by sequential cycles or stages. Down to a depth of $h_1 = d_f^2/\lambda \sim 1$ mm, laser radiation propagates in the slot according to the laws of geometric optics, while subsequent propagation proceeds in a waveguide regime with multiple reflections from three walls (Gladush & Smurov, 2011).

Let us assume that, before removal of a film of melted metal from the slot, its average temperature $<T_f>$ reaches a level of $<T_f> = (T_c'' - T_c')/2 = 2450$ K, where $T_c' = 1850$ K and $T_c'' = 3100$ K are the steel melting and boiling temperatures, respectively. Then, according to the energy balance of laser radiation, the power spent for cutting metal at speed v_c through $b \times h$ slot size (which includes the heating to T_c', supplying heat of fusion Λ', and heating the outer metal layer to a temperature close to T''), amounts to $Q_p = S_v \cdot h \cdot b \cdot v_c \approx 8.1$ W, where $h = 8$ mm, cutting speed $v_c \sim 1$ mm/s, and $S_v = \{\rho_c \cdot [c_c \cdot (T_c' - T_0) + \Lambda'_c]\} + \rho_l \cdot c_l \cdot (<T_f> - T_c') \approx 12 \cdot 10^9$ J/m^3 is the volume density of energy spent for heating steel from the initial temperature T_0 to $<T_f>$ and for its melting.

The time-averaged power of laser radiation supplied to the surface of a steel sheet is $<P_l> = 310$ W at a laser pulse power of $P_l = 930$ W. Therefore, according to the experimental data, the efficiency η_e of fiber-laser cutting with deep channeling (defined as $\eta_e = Q_p/<P_l>$ or $\eta_e = S_v/w_l$) amounts to 2.6%. This efficiency is determined by the product of the efficiency η_t of single-mode laser radiation transport in the waveguide regime, coefficient η_a of radiation absorption by the metal surface ($\eta_a = 30$—45% for $\lambda \sim 1$ μm) (Tsar'kova, 2004), and the fraction ε of heat losses in the cut zone. These thermal losses are mostly related to thermal conduction in four directions over a characteristic distance of $\sqrt{4 \cdot <\chi_c> \cdot \tau_{rad}} \approx 350$ μm. Estimations show that a liquid metal film prior to its removal accumulates $4.8 \cdot 10^{-2}$ J and the thermal losses amount to $11 \cdot 10^{-2}$ J, which corresponds to $\varepsilon \approx 0.7$. In this case, the efficiency of single-mode laser radiation transport is $\eta_t \approx \eta_e / [\eta_a (1 - \varepsilon)] \approx 0.25$ for $\eta_a = 0.35$.

After removal of the liquid metal film and switch-off of laser radiation, the heated region exhibits cooling within a time of $\tau_2 = \tau_1 - \tau_{rad} = 5.5$ ms over a characteristic distance of ≈500 μm. The established temperature, as estimated from the energy balance with allowance for removal of the liquid metal film, is ≈400 K**.** This is the initial metal temperature T_0 on the "step" (trough or shelf) before its subsequent heating, which enters into the formula for calculating S_v.

The experimental fact of the absence of precise cutting in the case of using few-mode fiber laser radiation is apparently related to a significantly lower efficiency of transporting this radiation to the cut zone.

The obtained results gave us the basis for developing a qualitative model of laser gas (oxygen) precision cutting with deep ($K \geq 30$) channeling. The main features of this model are as follows.

In the upper zone of the cut surface within depth h_1 ($K \sim 20$) the material is cut in the standard regime of laser gas cutting (Gladush & Smurov, 2011; Malikov et al., 2012). For $K \geq 30$, the static gas pressure in the near-wall jet is close to atmospheric (isobaric jet), and the large hydraulic losses of pressure (proportional to $\sim h/b$) together with jet divergence (in proportion to $\sim 1/z$) with allowance for gas heating lead to several-fold decrease in the initial subsonic gas flow velocity (to ~50 m/s) and dynamic pressure (to $\leq 10^3$ Pa) (Panchenko, 2009; Vitshas et al., 2014). In this case, the removal (blowing away) of melted metal from the "step" surface can only be ensured by creating a pressure pulse similar to that in the case of laser welding (Kaplan, 1994). Therefore, the process of laser cutting must proceed in a periodic-pulsed regime, in which the formation of a layer of liquid metal with thickness Δz_1 on the surface of "step" with dimensions $\Delta x \cdot b$ takes place rather slowly (within several microseconds, see below) while its subsequent removal (blowing away) is much (ten fold) faster. Experiments showed that, after blowing away the liquid layer, the irradiation must be interrupted until restoration of the initial conditions of cutting.

In the waveguide propagation zone, the intensity of radiation absorbed by the uppermost metal layer in a "step" is $I_w = P_l \cdot \eta_t \cdot \eta_a \cdot (1 - \varepsilon)/(\Delta x \cdot b) \approx 1.3 \cdot 10^5$ W/cm^2, which is lower by two orders of magnitude than the value necessary for the onset of intense metal evaporation observed, e.g., in laser welding, but is quite sufficient for effective heating of the metal (Gladush & Smurov, 2011; Kaplan, 1994; Goncharov et al., 2010).

Estimation of the density of a heat flux to the slot wall, as determined by heterogeneous reactions of iron oxidation $Fe + 1/2 \cdot O_2 \leftrightarrow FeO$ (with a thermal effect of 4.8 MJ/kg) and the oxidation of impurities gives, even provided complete consumption of oxygen flow in the slot (where its density and velocity are small), a value on the order of $\sim 10^4$ W/cm^2. This is more than ten times lower compared to the density of absorbed laser radiation (Smirnov, 2009).

The characteristic time τ_h of steel heating and melting on the "step" with thickness Δz_1, where the metal is heated from the initial temperature T_0 to the surface temperature T^* close to (but still lower than) the boiling temperature

T'', was estimated from the energy balance $S_v\cdot\sqrt{(4\cdot<\chi_m>\cdot\tau_h)}=I_w\cdot\tau_h$ and amounted to $\tau_h=4\cdot<\chi>\cdot(S_v/I_w)^2\approx 2.6$ ms ($<\chi>=0.65\cdot10^{-5}$ m^2/s), which is close to the radiation pulse duration τ_{rad}.

Let us consider the mechanism of pressure pulse formation in the gas mixture. Heating of a near-surface layer of the liquid metal to temperature T^* leads to the volume boiling of impurities (Cr, Cu, Ni, Si, S, As), the boiling temperatures of which are lower than that of iron and, probably, of dissolved gases (Goncharov et al., 2010). The resulting vapor flow sprays liquid particles (melt droplets with predominant iron content) against the heated (≈1000 K) oxygen flow. The particle size distribution is bimodal (Goncharov et al., 2010): the average particle size in the fine fraction is d_{s1} = 60 nm at a concentration of $N_{s1} \approx 10^{12}$ cm^{-3}, while coarse particles have an average diameter of d_{s2} = 10 μm.

Small-size particles occurring in the radiation field are evaporated within a time of $\tau_{s1}\sim(\rho_{liq}\cdot\Lambda''_{liq}\cdot d_{s1})/(3\cdot\eta_a\cdot P_l)\approx 0.2$ μs (for $\eta_a\approx 0.35$), while coarse particles are evaporated for ~100 μs. The resulting vapor has a temperature close to T'' = 3100 K and a concentration of iron atoms $\approx 9\cdot10^{18}$ cm^{-3}. Components of the vapor—gas phase of the two-phase system are mixed within $\tau_{mix}\sim (l_s)^2/\chi_v\sim 10$ ns (for $l_s\sim 1/(N_{s1})^{1/3}\sim 1$ μm) and acquire a temperature of ≈2000 K at a pressure of ≈0.4 MPa. The "hot" vapor—gas mixture of fuel and oxidant features exothermal reactions of oxidation of iron and impurities with characteristic time $\tau_{ox}\approx 5\cdot10^{-8}$ s (Smirnov, 2009), which is smaller than the time of establishment of atmospheric pressure $\tau_a\approx\Delta x/c_s\approx 0.3$ μs (where c_s is the velocity of sound).

Calculations in the approximation of thermodynamic equilibrium give a hot mixture temperature of 3480 K and a composition that includes a condensed FeO phase (with a mass fraction of ≈60%) and FeO vapor phase (≈4%), condensed Fe_3O_4 phase (6%), and vapor of impurities (M_i = C, Cr, Ni, Cu, Mn, Si) and/or their oxides (M_iO and M_iO_2) with molar fractions from 0.1% to 0.5%.

However, the condensation of FeO and Fe_2O_3 vapors does not take place in the field of intense laser radiation, although their boiling temperatures are ≈3700 K. Their presence in the vapor phase leads to an increase in the pressure up to 0.74 MPa. Moreover, the appearance of FeO molecules with strongly excited lower electron levels and significantly broadened absorption lines in the gas phase must apparently lead to intense absorption of the laser radiation with λ = 1.07 μm. Rapid quenching of the excited levels of FeO molecules leads to an increase both in the temperature of the vapor—gas mixture (up to ≈5000 K), which is limited by the dissociation of FeO molecules (dissociation energy, ≈49 kK), and in the pressure (up to 1.1 MPa). At this moment of time, the radiation must be switched off (as will be explained below) for a time that is necessary for restoration of the initial state of medium above the metal surface.

The pressure jump in the gas cap with dimensions $\Delta x\cdot b\cdot\Delta z_g$ (where $\Delta z_g\sim b$) leads to the formation of a shock wave (compression wave) with a Mach number of $M\approx 2$ and a cocurrent flow of mixture behind this wave at an initial velocity of ≈700 m/s against the oxygen flow and laser radiation propagation (Abramovich, 1976). The height and time of gas phase elevation are ~1 mm and ~20 μs, respectively.

The size of the "hot" gas cap above the liquid film, its pressure p_{cap}, and temperature vary while the cap exists for a time of $\tau_{imp}>\tau_a$. This pressure creates an average force impulse $<F_f\cdot\tau_{imp}>$ (where $F_f=p_{cap}\cdot\Delta x\cdot b$), which pushes the liquid film with volume $V_f=\Delta x\cdot\Delta z_1\cdot b$ and mass $m_f=\rho_f\cdot V_f$ toward the open end of the slot (along axis x) with velocity u_f. The characteristic velocity $<u_f>$ was estimated from the equation $m_f\cdot du_f/dt = F_f$ and amounted to $<u_f> = <p_{cap}>\cdot\tau_{imp}/(\rho_f\cdot\Delta z_1)\approx 0.3$ m/s, while the time of liquid film removal (blowing away) was estimated as $\tau_f\sim\Delta x/(2\cdot<u_f>)\approx 0.3$ ms, so that $\tau_f<<\tau_{rad}$. During removal of the liquid film, it exhibits disintegration into drops of various dimensions, most of which are carried away by the oxygen flow. Experiments showed that the remaining drops formed a small amount of agglomerated slag that was retained inside the slot.

In order to determine the velocity u_s of large particles with average diameter d_{s2} = 10 μm, we used the equation $m_s\cdot du_s/dt = F_s$, where $F_s = 3\pi\cdot C_o\cdot\eta\cdot d_{s2}\cdot\Delta u_s$, is the drag force, m_s is the particles mass, $C_0=21.1/Re_s+6.3/\sqrt{Re_s}+0.25>1$ is the resistance coefficient, $\Delta u_s=V-u_s$ is the relative velocity of particles (where the sign of u_s can either coincide with or be opposite to that of velocity V of the vapor–gas phase), $Re_s=\rho\cdot\Delta u_s\cdot d_{s2}/\eta$, η is the viscosity, $We = d_{s2}\cdot\rho\cdot(\Delta u_s)^2/\sigma_l << 1$ is the Weber criterion, and $\sigma_l\approx 1.7$ J/m^2 is the surface tension of iron. A solution of this equation with the corresponding initial and boundary conditions in the field of velocities of the ascending flow of the vapor–gas mixture yields a particle velocity of ≈10 m/s and an elevation height of ≈0.1 mm.

The nonstationary mixing of counter propagating flows of oxygen and a two-phase mixture of reaction products with different temperatures and densities in the slotted channel with developed surface roughness ($2\cdot k_s/b\sim 0.1$) over a length of several millimeters within a time on the order of $\sim10^{-5}$ s leads to the formation of a large-scale vortex flow structure with small velocity of directional flow toward the "step" surface. After termination of the concurrent flow of the vapor–gas phase, the inertial elevation of particles continues for ≈0.5 ms until their stopping

at a height of ≈3 mm. Then the particles are driven down to the "step" surface and carried toward the open end of the slot by the vortexed flow of predominantly oxygen for a time of ≈4 ms (as estimated from the force impulse equation). Thus, only a small velocity (~1 m/s) of the directional removal of products of the interaction of laser radiation and oxygen jet with metal allows the calculated time (4.5 ms) to be consistent with experimentally determined duration of the necessary pause of irradiation.

If the laser radiation is not switched off upon the pressure pulse formation, then relatively slow (with several tens of microseconds) heating and developed evaporation of coarse particles begins in the field of radiation with power density on the order of ~10^6 W/cm^2. The resulting mixture apparently features the optical discharge that propagates in the direction opposite to that of the optically transparent oxygen flow. This leads to the formation of an extended plasma cloud and the scattering and absorption of laser radiation. As a result, the transport of radiation energy significantly decreases and precision laser gas cutting process ceases.

4. Conclusion

The present investigation allowed us to obtain new scientific and technological results and led to the following main conclusions:

(i) Using radiation of a single-mode fiber laser with a power of 1 kW and oxygen as the cutting gas, it is possible to realize the process of deep channeling ($K \geq 30$) and obtain slotted holes of arbitrary shape with widths up to ≈60 μm and large calibers (up to 60) in low-carbon steel sheets;

(ii) Precision fiber-laser cutting of low-carbon steel with deep channeling ($K \geq 30$) is possible only with oxygen as the cutting gas, which means that the process has a clearly pronounced laser-thermochemical character; the action of oxygen varies with depth of region in the cut and is principally differs from the case of CO_2 laser cutting;

(iii) The removal of liquid metal from the cut takes place under the action of a pressure pulse, which is created as a result of evaporation of a small-size fraction of liquid particles in the field of laser radiation, reaction of iron oxidation in the vapor—gas phase, and heating of iron oxide in the gas phase during an isochoric process;

(iv) Precision cutting is only realized in a periodic-pulsed regime of fiber laser operation with optimum on/off ratio and pulse repetition rate;

(v) The cut surface exhibits a periodic structure of solidified metal melt in the form of a "hill—trough" relief pattern with a step of 120—270 μm (depending on the depth) in the direction of cutting; in addition, the relief contains small-scale (~10 μm) cone-shaped cones and craters;

(vi) Precision fiber laser cutting leads to a small increase in the cut surface hardness, not exceeding 20% as compared to the initial (unprocessed) surface and 50% as compared to the value inside the sheet, so that the properties of steel change only slightly relative to the initial values;

(vii) The efficiency of precision single-mode fiber laser cutting of large-caliber slotted holes does not exceed 3%, while the efficiency of radiation transport to the cut zone in the waveguide regime does not exceed 25% at a coefficient of radiation absorption by the metal $\eta_a \approx 0.35$. The useful specific radiation power deposition during single-mode fiber laser cutting is $w_l \approx 7 \cdot 10^{11}$ J/m^3 (to within 20%) for all thicknesses of low-carbon steel sheet up to 10 mm.

Acknowledgments

The authors are grateful to V.M. Plotnikov, I.G. Rudoi, and R.A. Checkryzev for fruitful discussions, valuable remarks, and help in work, and L.A. Koroleva, L.F. Solov'eva, and A.V. Zhukov for carrying out computations and processing experimental data.

This study was supported in part by the Foundation for Promotion of the Development of Small Business in Science and Technology in Russia, project no. 8372r/13353 of September 14, 2010.

References

Abramovich, G. N. (1976). *Applied gasdynamics (in Russian)*. Moscow: Nauka.

IPG in the News. (2014). In *IPG Pthotonics, The Power to Transform*. Retrieved from www.ipgphotonics.com/news_ipg_htm

Gladush, G. G., & Smurov, I. (2011). *Physics of laser materials processing: Theory and experiment.* Berlin-Heidelberg: Springer-Verlag.

Goncharov, V. K., Kozadaev, K. V., Popechits, V. I., &Puzyrev, M. V. (2010). Studying the effect of high-energy radiation on matter for creating novel materials and technologies *(in Russian)*. *Vestnik Belarus Gos.Universiteta* (No. 1, pp. 1-10). Retrieved from http://elib.bsu.by/handle/123456789/2065

Kaplan, A. (1994). A model of deep penetration laser welding based on calculation of the keyhole profile. *J. Phis. D: Appl. Phys., 27*, 1805-1814. Retrieved from www.sciencedirect.com/science/article/pii/S187538921300117%

Malikov, A. G., Orishich, A. M., & Shulyat'ev, V. B. (2012). Energy characteristics of laser oxygen cutting of steel by radiation of CO_2 laser *(in Russian). Quantum Electronics, 42,* 640-644.

Morgenthal, L. (2012). *Cutting with fiber lasers*. Paper presented at the 1st International Fraunhofer Workshop on Fiber Lasers, Dresden, Germany. Retrieved from ftp://194.87.10.34/.../mor_scheiden mit faserlasern_02.pdf

Smirnov, V. N. (2009). Interaction of Iron Atoms with Molecular Oxygen *(in Russian)*. Retrieved from www.chemphys.edu.ru/pdf/2009-06-08-001.pdf

Trumpf Co. (2012). Technological laser complexes based on CO_2 lasers and ytterbium SLEB lasers of Trumpf Co. Retrieved from http://www.ru.trumpf.com

Tsar'kova, O. G. (2004). Optical and thermophysical properties of metals, ceramics, and diamond films under high-temperature laser heating *(in Russian).* Retrieved from http://www.gpi.ru/trudiof/vol_60.php

Vitshas, A. A., Zelentsov, A. G., Lopota, V. A., Menakhin, V. P., Panchenko, V. P., & Soroka, A. M. (2014). Features of precision slot cutting with a large number of calibers using the radiation of a single-mode fiber laser. *Doklady Physics, 59,* 79-85. http://dx.doi.org/10.1134/S1028335814020049